A new manganese-based single-molecule magnet with a record-high antiferromagnetic phase transition temperature*

Cui Yan(崔 岩), Li Yan-Rong(李艳荣), Li Rui-Yuan(李瑞元), and Wang Yun-Ping(王云平)†

Beijing National Laboratory for Condensed Matter Physics, Institute of Physics, Chinese Academy of Sciences, Beijing 100190, *China*

(Received 27 March 2013; revised manuscript received 3 April 2013; published online 20 April 2014)

We perform both dc and ac magnetic measurements on the single crystal of $Mn_3O(Et\text{-}sao)_3(ClO_4)(MeOH)_3$ single-molecule magnet (SMM) when the sample is preserved in air for different durations. We find that, during the oxidation process, the sample develops into another SMM with a smaller anisotropy energy barrier and a stronger antiferromagnetic intermolecular exchange interaction. The antiferromagnetic transition temperature observed at 6.65 K in the new SMM is record-high for the antiferromagnetic phase transition in all the known SMMs. Compared to the original SMM, the only apparent change for the new SMM is that each molecule has lost three methyl groups as revealed by four-circle x-ray diffraction (XRD), which is thought to be the origin of the stronger antiferromagnetic intermolecular exchange interaction.

Keywords: single-molecule magnet, quantum tunneling of magnetization, antiferromagnetic intermolecular exchange interaction

PACS: 75.50.Xx, 76.60.Es, 75.30.Et, 75.30.Kz **DOI:** 10.1088/1674-1056/23/6/067504

1. Introduction

Single-molecule magnets (SMMs) are a new kind of organic magnetic material, which have attracted much attention since the first SMM Mn_{12} was found in 1993.[1] The magnetization relaxation time of SMMs is extremely long at low temperature[2] due to the high magnetic anisotropy energy barrier. On the other hand, they also exhibit an impressive quantum effect, quantum tunneling of the magnetization (QTM) below blocking temperature.[3,4] With these properties, SMMs are considered to be good candidates for quantum computing, high-density information storage,[5,6] and other functional magnetic materials.[7,8]

SMMs with intermolecular exchange interaction have raised special interest due to the different quantum behaviors observed in them. Recently, a lot of works were reported[9–14] for different QTM phenomena found in these SMMs, and a long-range magnetic order has been observed in some of the systems such as Mn_4[13] and Ni_4.[14] However, in the reported studies, either the QTM phenomenon is not apparent, or the phase transition temperature is quite low. In this paper, we report both dc and ac magnetic measurements on a single crystal of Mn_3 SMM (with identical antiferromagnetic exchange interaction in its *ab* plane[12]) during an oxidation process. We find that the sample develops into a new SMM in the oxidation process, and the new SMM displays an apparent QTM as well as a record-high antiferromagnetic transition temperature which excels all known SMMs. Therefore, the new Mn_3 SMM should be a very good candidate for investigating the effect of the long-range order on QTM in SMMs.

2. Method

The single crystal of single-molecule magnets (SMMs) Mn_3 ($[Mn_3O(Et\text{-}sao)_3(ClO_4)(MeOH)_3]$) is synthesized according to the reported method.[15–17] Mn_3 is an SMM with antiferromagnetic intermolecular exchange interaction in *ab* plane.[15] In *c* direction (easy axis), the intermolecular interaction force is the van der Waals' force, which is much weaker. Therefore, Mn_3 has a two-dimensional magnetic structure. The Hamiltonian of Mn_3 can be described as follows:

$$\hat{\mathscr{H}} = -D\hat{S}_z{}^2 - g\mu_B\mu_0 H_z\hat{S}_z - J\sum_{i=1}^{3}\hat{S}_{iz}\hat{S}_z, \qquad (1)$$

where the first term represents the zero-field splitting energy, which produces a uniaxial anisotropy barrier separating opposite projections of the spin along the magnetic easy axis. The second term is the Zeeman energy under an applied field. The third term is the intermolecular exchange interaction energy between one molecule and its neighbors. For fresh Mn_3,[12] $D \gg |J|$ and the value of J is negative and hence it may be described by two-dimensional antiferromagnetic Ising model. However, within the range of our measuring temperature, the antiferromagnetic interaction is too weak to form antiferromagnetic phase. The dc and ac magnetic susceptibility measurements of Mn_3 are performed using a 7T SQUID-VSM (Quantum Design) and 14T PPMS (Quantum Design), respectively.

*Project supported by the National Key Basic Research Program of China (Grant No. 2011CB921702) and the National Natural Science Foundation of China (Grant No. 11104331).

†Corresponding author. E-mail: ypwang@iphy.ac.cn

© 2014 Chinese Physical Society and IOP Publishing Ltd

3. Results and discussion

Figure 1 shows the magnetization versus temperature (M–T) curves of Mn_3 preserved in air on different days. In the field of SMMs, the definition of the blocking temperature T_B is at the inflection point of the zero field-cooling (ZFC) curve. For fresh Mn_3 (hereafter Mn_3(I)), the blocking temperature is $T_B = 3.15$ K (which depends on the height of anisotropy energy barrier) shown in Fig. 1(a). Comparing Figs. 1(a), 1(b), and 1(c), it is seen that, as time goes by, with temperature decreasing, a drop in the M–T curve appears gradually as shown in Fig. 1(b), and eventually the drop becomes apparent and stable, with the blocking temperature T_B observed to be 2.76 K as shown in Fig. 1(c). The heat capacity curves at different fields are shown in Fig. 1(d). It is seen that the peak moves to a lower temperature with the field increasing, which is characteristic of the antiferromagnetic phase. The antiferromagnetic phase transition temperature T_N is seen to be 6.65 K at zero field in Fig. 1(d), which is consistent with the corresponding temperature where the M–T curve starts dropping with decreasing temperature, as shown in Fig. 1(b), as well as the corresponding temperature where the steep drop of the M–T curve occurs while the temperature is decreasing, as shown in Fig. 1(c). Thus, it demonstrates that the drop observed in M–T curves resulted from the antiferromagnetic phase transition. These results indicate that the Mn_3(I) develops into another SMM (hereafter Mn_3(II)) with much stronger antiferromagnetic intermolecular exchange interaction and smaller anisotropy energy barrier when it is preserved in air. Our follow-up studies on Mn_3(II) have confirmed that it is a stable system and its magnetic properties can stay unchanged for years.

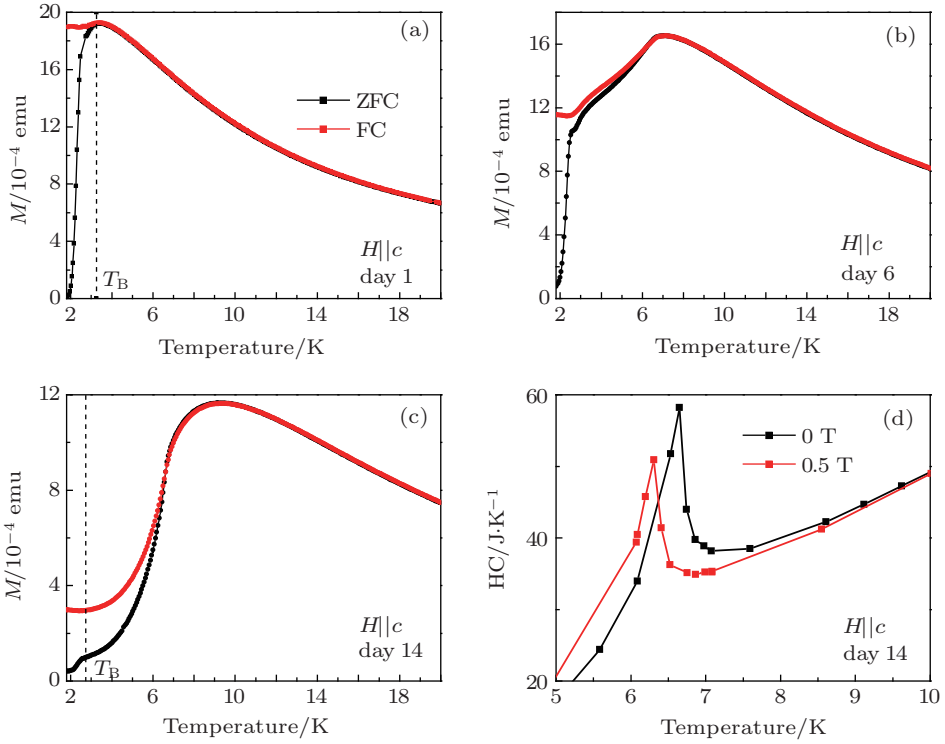


Fig. 1. (color online) (a) The dc magnetization versus temperature curves of fresh Mn_3 during field-cooling (FC) and zero field-cooling (ZFC) processes. (b) The FC and ZFC curves of the same sample preserved in air on day 6. (c) The FC and ZFC curves of the same sample preserved in air on day 14. The magnetic field is parallel to the easy axis (c axis). The applied field is 100 Oe (1 Oe = 79.5775 A·m^{-1}). (d) The heat capacity (HC) curves of the same sample preserved in air on day 14 at different fields.

The normalized magnetization hysteresis loops of Mn_3 preserved in air are demonstrated in Fig. 2. It is seen that the shape of the hysteresis loops becomes narrower as the days move on, which suggests the anisotropy energy barrier gets smaller. On the other hand, the quantum tunneling of the magnetization steps are seen on the hysteresis loops and the first step deviates from zero magnetic field due to the antiferromagnetic intermolecular exchange interaction.[18] It is also seen that, with the days advancing, the quantum tunneling of the magnetization steps of Mn_3(I)[12] are gradually succeeded by a new series of quantum tunneling of the magnetization steps of Mn_3(II). The position of the first quantum tunneling of the magnetization step (labeled by the blue dashed line in Fig. 2) of Mn_3(II) moves to a higher field compared with the Mn_3(I) (labeled by the black dashed line in Fig. 2), which indicates that the antiferromagnetic intermolecular exchange interaction becomes stronger. The result is consistent with the results from the M–T experiments. It should be noted that, for a certain period of time during the process, Mn_3(I) and Mn_3(II) are coexistent, which means the two kinds of antiferromagnetic exchange interaction are coexistent.

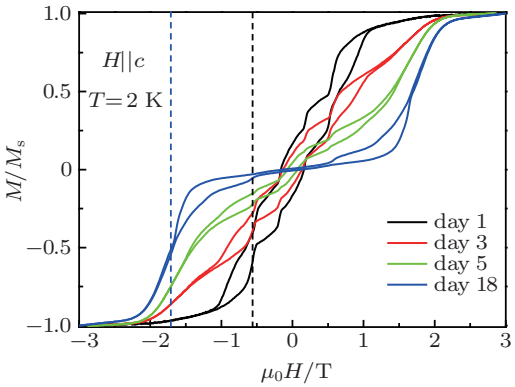


Fig. 2. (color online) Normalized hysteresis loops at 2 K of Mn_3 preserved in air on different days. The magnetic field is parallel to the easy axis (*c* axis). The sweep rate is 50 Oe/s. The first QTM step of the sample on day 1 and day 18 are labeled by dashed lines with corresponding color.

The ac magnetic measurements of Mn_3 preserved in air on different days are performed on PPMS (Quantum Design). The results are shown in Fig. 3. The real component curves (χ'–T) and imaginary component curves (χ''–T) of Mn_3(I) at different frequencies are shown in Figs. 3(a) and 3(b). It is seen that the peaks of both χ'–T and χ''–T curves move to higher temperature direction with the frequency increasing, which is an ordinary characteristic for the spin-flip relaxation of SMM due to the magnetic bistability. By the Arrhenius law for the relaxation time τ:[19]

$$\tau = \tau_0 \exp\left(\frac{U_{\text{eff}}}{k_{\text{B}}T}\right), \tag{2}$$

we can get the effective energy barrier of Mn_3(I) is 56.4 K, with fitting curve shown in Fig. 3(c). On the other hand, the χ'–T curves and the χ''–T curves of Mn_3(II) at different frequencies are shown in Figs. 3(d) and 3(e). The peaks of χ'–T curves do not move as the frequency increases, which may be a characteristic of antiferromagnetic phase transition. Meanwhile, the χ''–T curves also exhibit the characteristic for the spin-flip relaxation of SMM, which means the Mn_3(II) is still an SMM. According to Eq. (2), the effective energy barrier of Mn_3(II) is calculated to be 43.4 K, with the fitting curve shown in Fig. 3(f). The results from ac measurements are consistent with those from dc measurements, which lead to the conclusion that Mn_3(II) is a kind of SMM with smaller effective energy barrier and stronger antiferromagnetic intermolecular exchange interaction compared to Mn_3(I). Note that, in the imaginary component curves, with frequency increasing, the peaks of χ'' are steeply going up for Mn_3(II) whereas slowly going down for Mn_3(I). The reason is that the height of the

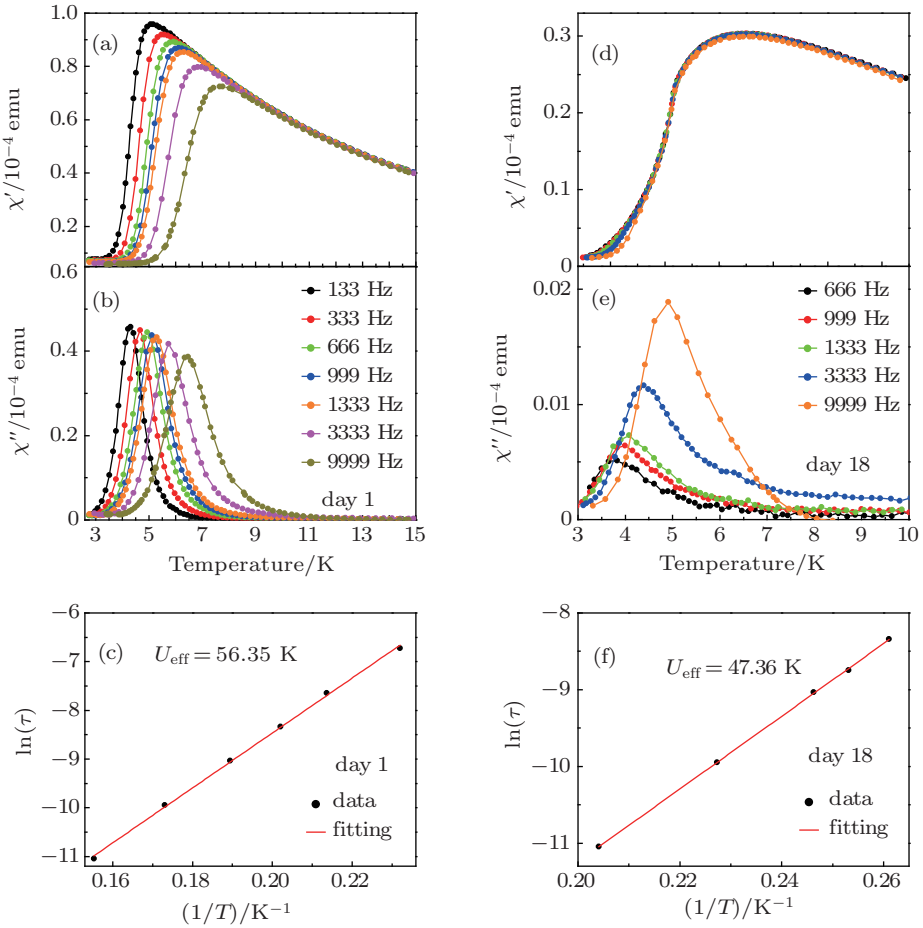


Fig. 3. (color online) (a) and (b) The real component (χ'–T) and imaginary component curves (χ''–T) of ac magnetic susceptibility at different frequencies of Mn_3(I), respectively. (c) The fitting curves of effective energy barrier of Mn_3(I) by Arrhenius law. (d) and (e) The χ'–T curves and χ''–T curves at different frequencies of Mn_3(II), respectively. (f) The fitting curves of effective energy barrier of Mn_3(II) by Arrhenius law.

peak of χ'' is proportional to the number of the molecules participating in the spin-flip process, the existence of the antiferromagnetic phase transition in Mn_3(II) makes most molecules frozen at low temperature. However, when the temperature is near the antiferromagnetic phase transition temperature these molecules will be unfrozen by the fluctuation which resulted in the peak of χ'' at high frequency being higher than that at low frequency.

In order to understand the nature of the different magnetic properties between Mn_3(I) and Mn_3(II), we need to look at the crystal structure[17] of them. The crystal structure is measured by four-circle x-ray diffractometer (Bruker SMART APEX-CCD) and the molecular structure is figured out by SHELXTL. We find that both Mn_3(I) and Mn_3(II) have the same lattice space group and symmetry. The apparent change takes place at the molecular structure as shown in Figs. 4(a) and 4(b). The Mn_3(II) molecule has lost three methyl groups which leads to the lattice constants being just slightly smaller. Besides, this change may have caused the antiferromagnetic intermolecular exchange interaction of Mn_3(II) to be stronger than that of Mn_3(I).[15]

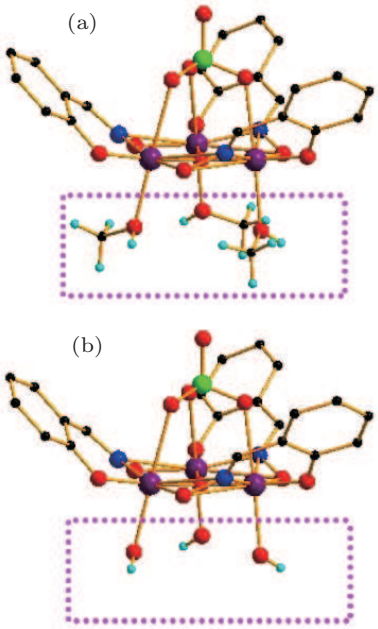


Fig. 4. (color online) (a) The molecular structure of Mn_3(I). (b) The molecular structure of Mn_3(II). The ethyl groups on Et-sao ligands[17] are omitted for clarity. Mn, purple; N, blue; O, red; Cl, green; C, black; H, cyan.

4. Conclusion

In conclusion, we have performed both dc and ac magnetic measurements on the single crystal of Mn_3 SMM preserved in air for different durations. We find that the fresh Mn_3 (Mn_3(I)) with weaker antiferromagnetic interaction develops into another SMM (Mn_3(II)) with stronger antiferromagnetic interaction. The latter shows an antiferromagnetic phase transition with a record-high transition temperature of 6.65 K. On the other hand, according to the results of ac magnetic measurements and dc magnetization hysteresis loops, the anisotropy energy barrier of Mn_3(II) is smaller than Mn_3(I). As revealed by four-circle XRD diffraction experiment, the only apparent change between Mn_3(I) and Mn_3(II) SMM is that each molecule of the Mn_3(II) SMM has lost three methyl groups, which may have caused the stronger antiferromagnetic interaction.[15] With these properties, Mn_3(II) should be a good candidate for studying the effect of intermolecular interaction on the quantum behavior, such as QTM and relaxation process, as well as the correlations between the magnetic properties and the lattice structure. Besides, the magnetic structure of Mn_3 can be described by using two-dimensional antiferromagnetic Ising model, which makes it much simpler and cleaner than normal magnetic systems[19–23] for studying multiple magnetic interaction and magnetic phase transition at low dimensions.[24]

References

[1] Sessoli R, Tsai H L, Schake A R, Wang S, Vincent J B, Folting K, Gatteschi D, Christou G and Hendrickson D N 1993 *J. Am. Chem. Soc.* **115** 1804
[2] Chrustou G, Gatteschi D, Hendrickson D N and Sessoli R 2000 *Mater. Res. Soc. Bull.* **25** 66
[3] Friedman J R, Sarachik M P, Tejada J and Ziolo R 1996 *Phys. Rev. Lett.* **76** 3830
[4] Henderson J J, Koo C, Feng P L, Barco E D, Hill S, Tupitsyn I S, Stamp P C E and Hendrickson D N 2009 *Phys. Rev. Lett.* **103** 017202
[5] Leuenberger M N and Loss D 2001 *Nature* **410** 789
[6] Ardavan A, Rival O, Morton J J L, Blundell S J, Tyryshkin A M, Timco G A and Winpenny R E P 2007 *Phys. Rev. Lett.* **98** 057201
[7] Bogani L and Wernsdorfer W 2009 *Nat. Mater.* **7** 179
[8] Xiong Z H, Wu D, Vardeny Z V and Shi J 2004 *Nature* **410** 821
[9] Wernsdorfer W, Alcalde A N, Hendrickson D N and Christou G 2002 *Nature* **416** 406
[10] Tiron R, Wernsdorfer W, Alcalde A N and Christou G 2003 *Phys. Rev. B* **86** 140407
[11] Wernsdorfer W, Bhaduri S, Tiron R, Hendrickson D N and Christou G 2002 *Phys. Rev. Lett.* **89** 197201
[12] Li Y R, Liu R Y, Liu H Q and Wang Y P 2014 *Phys. Rev. B* **89** 184401
[13] Miyasaka H, Nakata K, Lecren L, Coulon C, Nakazawa Y, Fujisaki T, Sugiura K, Yamashita M and Clérac R 2006 *J. Am. Chem. Soc.* **128** 3770
[14] Zuo J W, Liu H Q, Li Y R, Su S K and Wang Y P 2012 *Sci. China: Phys. Mech. Astron.* **55** 11
[15] Inglis R, Taylor S M, Jones L F, Papaefstathiou G S, Perlepes S P, Datta S, Hill S, Wernsdorfer W and Brechin E K 2009 *Dalton Trans.* **42** 9157
[16] Inglis R, Papaefstathiou G S, Wernsdorfere W and Brechin E K 2009 *Aust. J. Chem.* **62** 1108
[17] Inglis R, Jones L F, Karotsis G, Collins A, Parsons S, Perlepes S P, Wernsdorfer W and Brechin E K 2008 *Chem. Commun.* 5924
[18] Boskovic C, Bircher R, Piggott T P L W, Güdel H U, Paulsen C, Wernsdorfer W, Barra A L, Khatsko E, Neels A and Evans H S 2003 *J. Am. Chem. Soc.* **125** 14046
[19] Luis F, Bartolome J, Fernandez J F, Tejada J, Hernández J M, Zhang X X and Ziolo R 1997 *Phys. Rev. B* **55** 11448
[20] Murakami Y, Yoo J H, Shindo D, Atou T and Kikuchi M 2003 *Nature* **423** 965
[21] Nishihara Y and Yamaguchi Y 1984 *J. Phys. Soc. Jpn.* **53** 2201
[22] Moreo A, Yunoki S and Dagotto E 1999 *Science* **283** 2034
[23] Semenov Y G, Zavada J M and Kim K W 2011 *Phys. Rev. B* **84** 165435
[24] Santos M A, Marques M C and Oliveira J M B 1988 *J. Phys. C: Solid State Phys.* **21** 747